

Water Oxidation | Hot Paper |

A Water-Soluble Copper–Polypyridine Complex as a Homogeneous Catalyst for both Photo-Induced and Electrocatalytic O₂ EvolutionRui-Juan Xiang,^[a, b] Hong-Yan Wang,^{*[a, b]} Zhi-Juan Xin,^[a, b] Cheng-Bo Li,^[c] Ya-Xing Lu,^[b] Xue-Wang Gao,^[d] Hua-Ming Sun,^[b] and Rui Cao^{*[b, e]}

Abstract: The water-soluble polypyridine copper complex [Cu(F₃TPA)(ClO₄)₂] (**1**; F₃TPA = tris(2-fluoro-6-pyridylmethyl)amine) catalyzes water oxidation in a pH 8.5 borate buffer at a relatively low overpotential of 610 mV. Assisted by photosensitizer and an electron acceptor, **1** also exhibits activity as a homogeneous catalyst for photo-induced O₂ evolution with a maximum turnover frequency (TOF) of $(1.58 \pm 0.03) \times 10^{-1} \text{ s}^{-1}$ and a maximum turnover number (TON) of 11.61 ± 0.23 . In comparison, the reference [Cu(TPA)(ClO₄)₂] [TPA = tris(2-pyridylmethyl)amine] displayed almost no activity under either set of conditions, implying the crucial role of the ligand in determining the behavior of the catalyst. Experimental evidence indicate the molecular catalytic nature of **1**, leading to a potentially practical strategy to apply the copper complex in a photoelectrochemical device for water oxidation.

Water oxidation has become one of the most attractive targets for the conversion of solar energy or electricity into chemical fuels.^[1] In comparison with heterogeneous systems, molecular catalysts are advantageous, since their redox and kinetic properties are, in principle, easily tunable by molecular design. No-

tably, with a wide choice of redox-active metal centers and set of ligands, earth-abundant cobalt, nickel, and iron complexes are interesting candidates, the oxygen evolving activity of which has prompted an opportunity to broaden the range of available catalysts through fundamental coordination chemistry.^[2] Inspired by the extensive biological and biomimetic activities of copper enzymes and complexes in nature,^[3] fundamental progress has been made in the development of copper-based models, some of which undergo facile and reversible O–O bond formation and cleavage.^[4] These efforts have led to an increasing focus on the application of copper complexes in water oxidation. To date, only a few copper species have been reported as molecular catalysts to enable electrocatalytic water oxidation,^[5] therefore practical strategies are required for a better design of robust, efficient and stable copper catalysts.

Artificial photosynthesis by catalytic oxidation of water is among the most-investigated technologies for solar-to-chemical energy conversion.^[6,7] Molecular catalysts increase the practicality of this process, because they facilitate the integration of chromophores or chromophore antennae. Moreover, their derivatives can be further functionalized assembly into photoelectrochemical devices. Owing to their relatively high stability and low light absorption, functionalization of copper complexes by well-defined coordination chemistry is a very appealing and promising strategy to develop catalysts for photo-induced water oxidation. Herein, we report a water-soluble copper polypyridine complex **1** (Figure 1), which functions as a molecular catalyst for water oxidation under both visible-light irradiation and electrochemical conditions. To our knowledge, it is the first such photochemical investigation of a copper catalyst for O₂ evolution and this result may allow a derivative to be incorporated into molecular assemblies for photoelectrochemical water oxidation.

The mononuclear copper polypyridine compound **1** was obtained as a light blue powder through direct coordination of a α -fluorinated tris(2-pyridylmethyl)amine^[8] (F₃TPA) with Cu(ClO₄)₂·6H₂O in acetonitrile. Complex **1** exhibits good solubility in both acetonitrile and water. The UV/Vis absorption spectrum in basic borate buffer (0.1 M, pH 9) displays a band at $\lambda \approx 260 \text{ nm}$ and a shoulder at $\lambda \approx 340 \text{ nm}$. Both absorption intensities are linearly dependent on the catalyst concentration (see the Supporting Information, Figure S1). The UV/Vis spectra of **1** in basic borate buffer when measured after 0, 4, 6, 8, and 18 h (see the Supporting Information, Figure S2) display identical absorptions for each measurement, supporting the notion

[a] R.-J. Xiang, Prof. Dr. H.-Y. Wang, Z.-J. Xin
Key Laboratory of Macromolecular Science of Shaanxi Province
School of Chemistry and Chemical Engineering
Shaanxi Normal University, Xi'an, 710119 (P. R. China)

[b] R.-J. Xiang, Prof. Dr. H.-Y. Wang, Z.-J. Xin, Y.-X. Lu, Dr. H.-M. Sun,
Prof. Dr. R. Cao
School of Chemistry and Chemical Engineering
Shaanxi Normal University, Xi'an, 710119 (P. R. China)
E-mail: hongyan-wang@snnu.edu.cn
ruicao@ruc.edu.cn

[c] Dr. C.-B. Li
College of Chemistry & Materials Science
Northwest University, Xi'an, 710127 (P. R. China)

[d] Dr. X.-W. Gao
Key Laboratory of Photochemical Conversion and Optoelectronic Materials,
Technical Institute of Physics and Chemistry
Chinese Academy of Sciences, Beijing, 100190 (P. R. China)

[e] Prof. Dr. R. Cao
Department of Chemistry, Renmin University of China
Beijing, 100872 (P. R. China)

Supporting information for this article is available on the WWW under
<http://dx.doi.org/10.1002/chem.201504066>.

that the monomeric structure of **1** is stable under these conditions. Complex **1** displays absorptions almost above $\lambda = 400$ nm, implying that **1** does not compete for visible-light absorption in the system containing chromophore. Vapor diffusion of Et₂O into an acetonitrile solution of **1** yielded light blue crystals suitable for X-ray diffraction (Figure 1). The Cu center is coordinat-

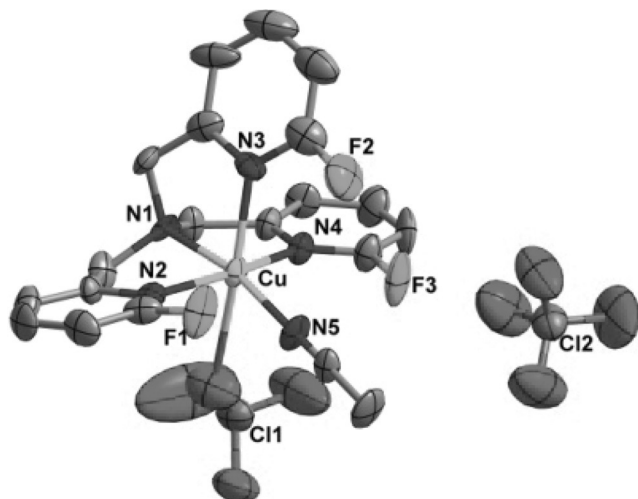


Figure 1. The crystal structure of **1** with thermal ellipsoids set at 50% probability level. Solvent molecules and hydrogen atoms are omitted for clarity.

ed by a F₃TPA ligand through four N atoms, an acetonitrile solvent molecule, and a ClO₄⁻ ion, to give a distorted tetragonal bipyramidal coordination geometry. The tertiary amine N atom and the acetonitrile N atom are located at the axial positions, whereas the three pyridine N atoms and the perchlorate O atom are in the equatorial plane.

In the presence of photosensitizer [Ru(bpy)₃](ClO₄)₂ and electron acceptor Na₂S₂O₈ with excitation at $\lambda = 470 \pm 10$ nm, photo-induced water oxidation of compound **1** was monitored by a Clark electrode. A pH 8.5 borate buffer was found to be optimal for the process (see the Supporting Information Table S1). A lower pH rendered photocatalysis much less efficient, whereas a higher pH gave rise to increased initial oxygen evolution rates and overall higher TONs but faster deactivation, demonstrating the decomposition of **1**. The concentration of buffer solution also influenced the activity, implying that O₂ formation preceded proton transfer with the basic buffer serving as the proton acceptor (Table S1).^[5d] Figure 2 shows photo-induced O₂ evolution versus time at various concentrations of **1** under the optimized conditions, where the arrow indicates the start of the irradiation. Due to accumulation of a steady-state concentration of the photogenerated intermediates, an initial lag time (ca. 9 s) was observed in the kinetic traces. The total amount of oxygen and the maximum turnover rate depended on the catalyst concentration. In the absence of **1**, a combination of [Ru(bpy)₃](ClO₄)₂ and Na₂S₂O₈ produced only a small amount of O₂; it is thus clear that **1** is required for efficient water oxidation. To make clear the contributions of the Cu catalyst to O₂ evolution, the TON and TOF

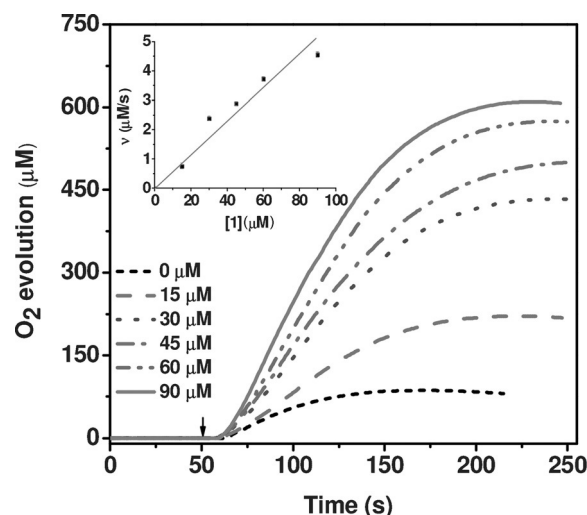


Figure 2. Light-induced water oxidation in a 1 mL reaction containing **1** (0 μM, 15 μM, 30 μM, 45 μM, 60 μM and 90 μM), [Ru(bpy)₃](ClO₄)₂ (0.4 mM), and Na₂S₂O₈ (5 mM) in borate buffer (75 mM, pH 8.5). The temperature of the Clark cell was kept constant at 20 °C, and the system was irradiated by using LEDs [$\lambda = (470 \pm 10)$ nm, 820 μEcm⁻²s⁻¹]. Inset: plot of oxygen generation initial velocities (v) vs. [**1**]. The rate v , is calculated in the linear part during the first 30 s of illumination and corrected for v when [**1**] = 0.

Table 1. TON and TOF (corrected for background oxygen solution activity) for the concentrations of **1** (without catalyst, [O₂] = 82 ± 2 μM).

Concentration of 1 [μM]	[O ₂] generated by 1 [μM]	TOF [s ⁻¹]	TON
0	–	–	–
15	137 ± 7	$(8.01 \pm 0.80) \times 10^{-2}$	9.06 ± 0.51
30	348 ± 7	$(1.58 \pm 0.03) \times 10^{-1}$	11.61 ± 0.23
45	397 ± 9	$(1.27 \pm 0.00) \times 10^{-1}$	8.94 ± 0.09
60	489 ± 6	$(1.18 \pm 0.02) \times 10^{-1}$	8.15 ± 0.11
90	515 ± 2	$(8.34 \pm 0.11) \times 10^{-2}$	5.72 ± 0.02

were calculated after correction for background in the absence of **1** (Table 1). Typically, the best condition, with TOF of $(1.58 \pm 0.03) \times 10^{-1}$ s⁻¹ and TON of 11.61 ± 0.23, was given by **1** at 30 μM. The initial velocities (v) of O₂ generation under the chosen conditions were then plotted versus [**1**] (Figure 2, inset), giving a linear fit with a rate constant $k = (6.42 \pm 0.30) \times 10^{-2}$ s⁻¹ at 20 °C. The first-order behavior with regard to [**1**] indicates a possible pathway for the O–O bond formation involving a highly oxidized Cu intermediate, which undergoes a rate-determining nucleophilic attack by a water molecular.^[2f,9] To test the influence of the fluoro substituents in the ligand, the reference complex [Cu(TPA)(ClO₄)₂] [**2**; TPA = tris(2-pyridylmethyl)amine] was synthesized. However, complex **2** proved almost inactive under the same conditions (see the Supporting Information, Figure S3).

To test whether the catalytic system was truly homogeneous in nature, the molecular integrity of **1** during photocatalysis was scrutinized by dynamic light scattering (DLS) experiments.^[2d,10] In a sample that had been illuminated for approximately 150 seconds, there was no evidence of any light scat-

tering that would have arisen from particle formation, suggesting that the system remained homogeneous during the illumination (see the Supporting Information, Figure S4). This point was further supported by Tyndall scattering analysis of the system containing **1** after photolysis (see the Supporting Information, Figure S5). Moreover, the solution was still transparent even after 2 days. In contrast, under the same conditions, although $\text{Cu}(\text{ClO}_4)_2$ also displayed activity, a white, cloudy precipitate was deposited from the solution, implying heterogeneity. Quite a similar occurrence was observed with $\text{Co}(\text{ClO}_4)_2$ as an alternative catalyst, consistent with the analysis obtained from DLS.^[11] A further difference of **1** from $\text{Cu}(\text{ClO}_4)_2$ is related to an attempted recycling experiment where fresh $[\text{Ru}(\text{bpy})_3]^{2+}$ and $\text{Na}_2\text{S}_2\text{O}_8$ were added to the illumination experiment when oxygen evolution had ceased (after ca. 150 s). For $\text{Cu}(\text{ClO}_4)_2$, due to the formation of copper oxide in the first run, the activity could be reinitiated with fresh $[\text{Ru}(\text{bpy})_3](\text{ClO}_4)_2$ and $\text{Na}_2\text{S}_2\text{O}_8$. However, only near-background activity was found in the case of **1**, indicating that intactness of **1** is required for O_2 evolution (see the Supporting Information, Figure S6).^[12] Together with differences in particle formation and deactivation behavior in the comparison of **1** with $\text{Cu}(\text{ClO}_4)_2$, these observations imply that **1** performs as a real catalyst for water oxidation. Interestingly, no CO_2 was detected in the system containing **1** after photolysis, and the decomposition products of **1** could be precipitated by adding concentrated NaOH to increase the pH to 11. These products were then analyzed by using ESI-MS (see the Supporting Information, Figure S7). A peak was detected at $m/z=263$, possibly attributable to the product with one pyridyl in F_3TPA detached from the copper center. It is assumed that axial open sites such as this facilitate metal oxidation and proton transfer during catalysis. Further signals appear at $m/z=425$ and 223, corresponding to $[\text{Cu}(\text{F}_3\text{TPA})(\text{OH})]^+$. Remarkably, the products remain bound to the Cu center, consistent with the lack of particle formation observed in this system.

Photo-induced water oxidation is based on electron transfer between all components. Therefore, steady-state emission spectroscopy was employed to acquire more insights into this process. On increasing the concentration of $\text{Na}_2\text{S}_2\text{O}_8$, the steady-state emission of excited $[\text{Ru}(\text{bpy})_3](\text{ClO}_4)_2$ in borate buffer solution was quenched with rate constant $k_q=9.8 \times 10^9 \text{ M}^{-1} \text{ s}^{-1}$ (see the Supporting Information, Figure S8). Meanwhile, during irradiation of $[\text{Ru}(\text{bpy})_3](\text{ClO}_4)_2$ with the electron acceptor $\text{Na}_2\text{S}_2\text{O}_8$, the absorption spectra show a decrease in the Ru^{II} MLCT band together with an increased absorption between 550 nm and 700 nm centered at 657 nm, reflecting the build-up of Ru^{III} species by electron transfer from excited $[\text{Ru}(\text{bpy})_3]^{2+}$ to $\text{S}_2\text{O}_8^{2-}$ (see the Supporting Information, Figure S9).^[2 g, 11a] Similarly, on addition of **1**, the steady-state emission of excited $[\text{Ru}(\text{bpy})_3](\text{ClO}_4)_2$ was quenched, with an increase in the concentration of Cu (see the Supporting Information, Figure S10). A smaller rate constant of $k_q=9.2 \times 10^8 \text{ M}^{-1} \text{ s}^{-1}$ was calculated from a Stern–Volmer plot (Figure S8). Therefore, we conclude that photocatalytic reaction is triggered by oxidative quenching of $[\text{Ru}(\text{bpy})_3]^{2+}$ on addition of $\text{Na}_2\text{S}_2\text{O}_8$. The resultant Ru^{III} species then oxidize the Cu^{II} complex to higher ox-

idation-state intermediates for subsequent water oxidation. This process is further supported by the observation of water oxidation in a mixture of **1** and $[\text{Ru}(\text{bpy})_3](\text{ClO}_4)_3$. As shown in Figure 3, in comparison to the background without **1**, the Cu

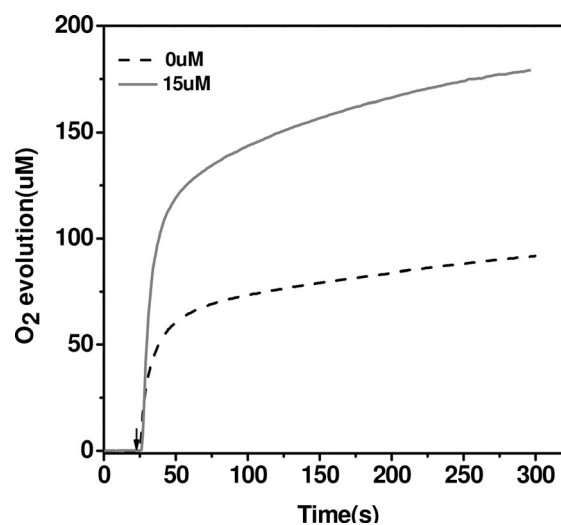


Figure 3. Water oxidation in a 1 mL reaction without or with **1** (15 μM) in the presence of $[\text{Ru}(\text{bpy})_3](\text{ClO}_4)_3$ (0.4 mM) in borate buffer (75 mM, pH 8.5). The temperature of the Clark cell was kept constant at 20 °C.

catalyst brought about an O_2 concentration of $92 \pm 4 \mu\text{M}$. Interestingly, a shorter lag time (< 2 s) and a faster O_2 evolution compared with the photolysis experiment occurred with an initial TOF of $(3.74 \pm 0.15) \times 10^{-1} \text{ s}^{-1}$ and a TON of 6.12 ± 0.25 with addition of 15 μM **1**, indicating that direct oxidation of **1** by $[\text{Ru}(\text{bpy})_3](\text{ClO}_4)_3$ led to an accelerated electron transfer (the TON and TOF were calculated after correction for background). Notably, this efficiency is also higher than that reported for $[(\text{bpy})\text{CuCl}_2]$ or $[(\text{bpy})\text{Cu}(\text{OH})_2]$ with $[\text{Ru}(\text{bpy})_3]^{3+}$ as the oxidant.^[5a, 13]

For a photoelectrochemical device, it is necessary to evaluate the electrocatalytic water oxidation activity of the catalyst. The electrochemical properties of **1** were therefore investigated and its capability for O_2 production was determined by controlled potential electrolysis (CPE) as follows. Using 1 cm^2 ITO (indium tin oxide) electrode as the working electrode, cyclic voltammetry of **1** was carried out in a 0.1 M pH 8.5 borate buffer under argon (Figure 4). The presence of **1** induced a large and irreversible oxidation wave at around 1.2 V vs. normal hydrogen electrode (NHE) and the current density reached up to 3 mA cm^{-2} , a great enhancement relative to the background. This pronounced electrochemical response can be explained by catalysis of water oxidation, demonstrating that **1** can perform as an electrocatalyst for O_2 evolution. In comparison, the much lower catalytic peak in the presence of **2** raised at 1.4 V. Besides, under the same condition, $\text{Ru}^{\text{III}}/\text{Ru}^{\text{II}}$ oxidation couple occurred at 1.31 V, positive shift with the potential for starting electrochemical water oxidation observed in the appearance of **1** (see the Supporting Information, Figure S11). Therefore, the Ru^{III} species generated by electron

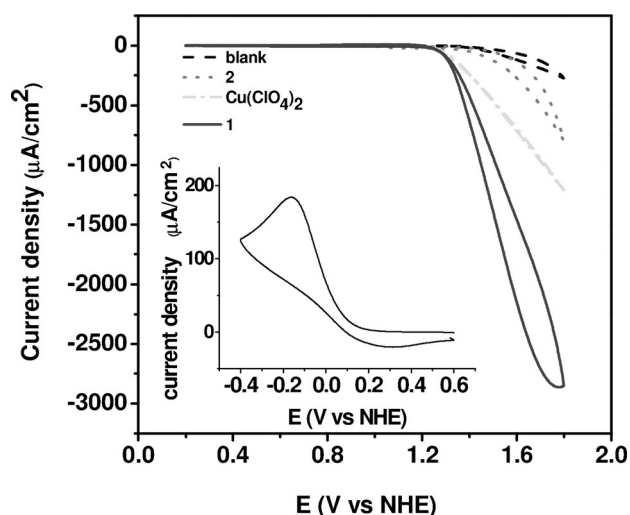


Figure 4. CVs of 1 mm **1** or $\text{Cu}(\text{ClO}_4)_2$ in a 0.1 M borate buffer at pH 8.5 with ITO (1 cm^2) as the working electrode at 50 mV s^{-1} . Inset: CV of 1 mm **1** at -0.4 V to 0.6 V .

transfer from photo-excited $[\text{Ru}(\text{bpy})_3]^{2+}$ to the electron acceptor is thermodynamically capable of promoting water oxidation with addition of **1**, but inhibited in the presence of **2**. This observation is consistent with the above experiments.

As shown in Figure 4, in pH 8.5 borate buffer, the onset of the catalytic wave with addition of **1** is around 1.34 V, which gives an overpotential of 610 mV,^[14] lower than that of previously reported copper complexes.^[5a,h] Although higher pH prompts the stronger catalytic current, accompanied by the decreasing overpotential based on the measurement at pH 7.1–9.0 (see the Supporting Information, Figure S12), pH 8.5 was chosen in order to retain conditions close to those of the photo-induced experiment.

From cyclic voltammetry measurements with the concentration of **1** ranging from 0 to 1 mM, the catalytic peak current (i_{cat}) varied linearly with $[\mathbf{1}]$ (see the Supporting Information, Figure S13). This first-order dependence is in line with a single-site mechanism for water oxidation catalysis according to Equation (1), where $n_{\text{cat}}=4$, representing the number of electrons transferred during water oxidation, F is Faraday's constant, A is the area of the electrode (in cm^2), $[C]$ is the catalyst concentration (in mol L^{-1}), k_{cat} is the catalytic rate constant, and D_{cat} is the diffusion coefficient of the catalyst (in $\text{cm}^2 \text{ s}^{-1}$).^[2c,5]

$$i_{\text{cat}} = n_{\text{cat}} F A [C] D_{\text{cat}}^{1/2} k_{\text{cat}}^{1/2} \quad (1)$$

Besides of catalytic peak of **1** in CV, a weak anodic wave at 0.27 V was induced with a cathodic wave at -0.11 V in the reverse scan ($\Delta E=380 \text{ mV}$ at 50 mV s^{-1} scan rate; Figure 4, inset). This process was assigned to the $\text{Cu}^{\text{II/I}}$ couple with $E_{1/2}=0.08 \text{ V}$.^[5d,h,15] The cathodic current density (i_d) varied linearly with the square root of the scan rate (see the Supporting Information, Figure S14). This result is consistent with the Randles–Sevcik relation given by Equation (2),^[5,16] where $n=1$, representing the electron transferred in the noncatalytic reaction,

ν is the scan rate, R is the gas constant, and T is the absolute temperature. Accordingly, D_{cat} can be determined from the slope of the line to be $1.74 \times 10^{-5} \text{ cm}^2 \text{ s}^{-1}$.

$$i_{\text{el}} = 0.4633 n F A [C] \left(\frac{n F \nu D_{\text{cat}}}{RT} \right)^{1/2} \quad (2)$$

The ratio of Equations (2) and (1), calculated with all of the constants, gives the simplified Equation (3) as follows:^[2c,5a,f,g]

$$\frac{i_{\text{cat}}}{i_{\text{el}}} = 1.38 \sqrt{\frac{k_{\text{cat}}}{\nu}} \quad (3)$$

k_{cat} established in this equation is usually considered as the apparent rate constant for a first-order or pseudo-first order O_2 evolution reaction. In electrochemistry, the TOF of a catalyst is usually referred to as the catalytic water oxidation rate constant k_{cat} . The electrocatalytic activity of **1** was estimated by plotting the catalytic current over the diffusive peak current i_{cat}/i_d as a function of the reciprocal of the square root of scan rate. With scan rates decreasing (see the Supporting Information, Figure S15), i_{cat}/i_d matches the trend from a pure diffusion behavior region to a pure kinetic behavior region.^[5g,16a] According to Equation (3), a TOF value of 0.38 s^{-1} can be calculated from the slope of the fitting line in Figure S13 (see the Supporting Information). Since the 4-electron water oxidation reaction is a complicated process, the calculated values can only be regarded as an estimate of the catalytic rate.

CPE experiments to evaluate the capability for water oxidation of **1** were conducted at 1.80 V on a 1.0 cm^2 surface-area ITO working electrode in a closed and deoxygenated electrolysis cell. In the presence of **1**, the catalytic charge was dramatically enhanced (Figure 5a). The background for oxygen formation at the applied potential in the absence of catalyst was negligible. During CPE, bubble evolution was clearly observed on the electrode surface (Figure 5b). After 2 h, the reaction headspace was analyzed by gas chromatography, and the result revealed that $41 \mu\text{mol}$ of O_2 had been produced with 8.2 catalytic turnovers based on the initial amount of **1** with a Fara-

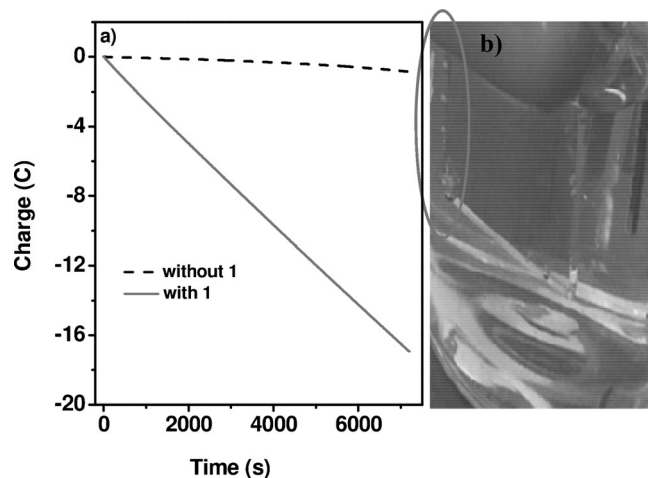


Figure 5. a) CPE with and without 1 mm **1** in a 0.1 M borate buffer (pH 8.5) at 1.8 V versus NHE; b) the bubbles on the electrode surface during CPE.

daic efficiency of approximately 93% (see the Supporting Information, Figure S16). The calculated Faradaic efficiency is somewhat lower, as some of the O₂ produced was solubilized in the electrolyte and not detected by headspace sampling.^[5c,d,f] Furthermore, the pH decreased by 0.3 after CPE, in accordance with consumption of OH⁻ by water oxidation.^[5f]

Several different techniques were used to establish whether any heterogeneous materials were produced during the reaction. Figure 5a shows the total charge passed during 2 h electrolysis, and the absence of an induction period at early electrolysis times implies homogeneous water oxidation catalysis.^[5d] In addition, UV/Vis spectra of the bulk solution containing **1** were measured before and after electrolysis, showing nearly identical absorption (see the Supporting Information, Figure S17). Moreover, SEM (scanning electron microscopy) was used to examine the morphology of the working electrode after electrolysis, giving very similar results to the bare ITO surface (see the Supporting Information, Figure S18a,b). Energy dispersive X-ray spectroscopy (EDS) also revealed that the electrode exhibited the same elemental composition as the bare ITO electrode after catalysis, implying that the decomposition of **1** could not have led to deposition of heterogeneous particles on the electrode (Figure S18c,d). After catalysis, the electrolyte solution was also examined by DLS, and no obvious signals were ascribed to particles, confirming no heterogeneity within the electrolyte mixture (see the Supporting Information, Figure S19). This was further supported by Tyndall scattering analysis (see the Supporting Information, Figure S20). The overall lack of evidence for particle formation, either adsorbed on the working electrode or present in the electrolyte solution, is collectively consistent with homogeneous catalysis.

It is usually considered that upon sequential oxidation of a metal catalyst in water by chemical, electrochemical or photochemical means, it is first converted into a molecular metal-oxo species or decomposing into a metal oxide prior to activating water oxidation.^[2d] The ligand plays a crucial role, particularly in determining the nature of the catalyst.^[17] It has been demonstrated that the TPA ligand is essential for binding firmly to the metal center to access the true catalytically active species.^[2g,12] Importantly, self-oxidation of the ligand in the oxidizing environment can be significantly diminished relaxed by electron-withdrawing fluoro substituents. Accordingly, it can reasonably be assumed that the stability of **1** as a molecularly well-defined homogeneous catalyst profits from the strong binding of the robust and oxidation-resistant F₃TPA ligand to the copper center.

In summary, a water-soluble copper complex bearing an F₃TPA ligand was synthesized and displayed water oxidation activity as a molecular catalyst under both photo-irradiated and electrochemical conditions. In spite of moderate catalytic behavior, the verification of a low-overpotential single-site copper molecular homogeneous catalyst, which is active under both electrochemical and photochemical conditions, opens up an opportunity for the development of stable molecular copper-based catalysts for water oxidation. More importantly, these developments can facilitate the ready incorporation of homogeneous catalysts into photoelectrochemical devices for

water oxidation, research into which is currently ongoing in our laboratory.

Acknowledgements

This work was supported by the National Natural Science Foundation of China (21402113), the Fundamental Research Funds for the Central Universities (6K201503033), and the "Thousand Talents Program" in China. We are grateful to Prof. Jing Liu at Shaanxi Normal University for providing access to the DLS instrument.

Keywords: copper · electrocatalysis · homogeneous catalysis · photochemistry · water oxidation

- a) J. J. Concepcion, J. W. Jurss, M. K. Brennaman, P. G. Hoertz, A. O. T. Patrocinio, N. Y. Murakami Iha, J. L. Templeton, T. J. Meyer, *Acc. Chem. Res.* **2009**, *42*, 1861–1870; b) H. Dau, I. Zaharieva, *Acc. Chem. Res.* **2009**, *42*, 1861–1870; c) R. Eisenberg, *Science* **2009**, *324*, 44–45; d) K. N. Ferreira, T. M. Iverson, K. Maghlaoui, J. Barber, S. Iwata, *Science* **2004**, *303*, 1831–1838; e) S. W. Kohl, L. Weiner, L. Schwartsburd, L. Konstantinovski, L. J. W. Shimon, Y. Ben-David, M. A. Iron, D. Milstein, *Science* **2009**, *324*, 74–77; f) B. Loll, J. Kern, W. Saenger, A. Zouni, J. Biesiadka, *Nature* **2005**, *438*, 1040–1044; g) D. G. Nocera, *Acc. Chem. Res.* **2012**, *45*, 767–776; h) R. D. L. Smith, M. S. Prevot, R. D. Fagan, Z. Zhang, P. A. Sedach, M. K. J. Siu, S. Trudel, C. P. Berlinguette, *Science* **2013**, *340*, 60–63; i) Y. Wu, M. Chen, Y. Han, H. Luo, X. Su, M.-T. Zhang, X. Lin, J. Sun, L. Wang, L. Deng, W. Zhang, R. Cao, *Angew. Chem. Int. Ed.* **2015**, *54*, 4870–4875; *Angew. Chem.* **2015**, *127*, 4952–4957.
- a) D. K. Dogutan, R. McGuire, Jr., D. G. Nocera, *J. Am. Chem. Soc.* **2011**, *133*, 9178–9180; b) J. L. Fillol, Z. Codola, I. Garcia-Bosch, L. Gomez, J. Jose Pla, M. Costas, *Nat. Chem.* **2011**, *3*, 807–813; c) Y. Han, Y. Wu, W. Lai, R. Cao, *Inorg. Chem.* **2015**, *54*, 5604–5613; d) C.-F. Leung, S.-M. Ng, C.-C. Ko, W.-L. Man, J. Wu, L. Chen, T.-C. Lau, *Energy Environ. Sci.* **2012**, *5*, 7903–7907; e) T. Nakazono, A. R. Parent, K. Sakai, *Chem. Commun.* **2013**, *49*, 6325–6327; f) E. Pizzolato, M. Natali, B. Posocco, A. M. Lopez, I. Bazzan, M. Di Valentin, P. Galloni, V. Conte, M. Bonchio, F. Scandola, A. Sartorel, *Chem. Commun.* **2013**, *49*, 9941–9943; g) H. Wang, Y. Lu, E. Miljngos, A. Thapper, *Chin. J. Chem.* **2014**, *32*, 467–473; h) D. J. Wasylenko, R. D. Palmer, E. Schott, C. P. Berlinguette, *Chem. Commun.* **2012**, *48*, 2107–2109.
- a) J. P. Klinman, *Chem. Rev.* **1996**, *96*, 2541–2562; b) E. I. Solomon, P. Chen, M. Metz, S.-K. Lee, A. E. Palmer, *Angew. Chem. Int. Ed.* **2001**, *40*, 4570–4590; *Angew. Chem.* **2001**, *113*, 4702–4724; c) E. I. Solomon, U. M. Sundaram, T. E. Machonkin, *Chem. Rev.* **1996**, *96*, 2563–2606.
- a) H. Hayashi, S. Fujinami, S. Nagatomo, S. Ogo, M. Suzuki, A. Uehara, Y. Watanabe, T. Kitagawa, *J. Am. Chem. Soc.* **2000**, *122*, 2124–2125; b) E. A. Lewis, W. B. Tolman, *Chem. Rev.* **2004**, *104*, 1047–1076; c) L. M. Mirica, X. Ottenwaelder, T. D. P. Stack, *Chem. Rev.* **2004**, *104*, 1013–1045; d) X. Ottenwaelder, D. J. Rudd, M. C. Corbett, K. O. Hodgson, B. Hedman, T. D. P. Stack, *J. Am. Chem. Soc.* **2006**, *128*, 9268–9269.
- a) S. M. Barnett, K. I. Goldberg, J. M. Mayer, *Nat. Chem.* **2012**, *4*, 498–502; b) Z. Chen, P. Kang, M.-T. Zhang, B. R. Stoner, T. J. Meyer, *Energy Environ. Sci.* **2013**, *6*, 813–817; c) Z. Chen, T. J. Meyer, *Angew. Chem. Int. Ed.* **2013**, *52*, 700–703; *Angew. Chem.* **2013**, *125*, 728–731; d) M. K. Coggin, M.-T. Zhang, Z. Chen, N. Song, T. J. Meyer, *Angew. Chem. Int. Ed.* **2014**, *53*, 12226–12230; *Angew. Chem.* **2014**, *126*, 12422–12426; e) W.-B. Yu, Q.-Y. He, X.-F. Ma, H.-T. Shi, X. Wei, *Dalton Trans.* **2015**, *44*, 351–358; f) M.-T. Zhang, Z. Chen, P. Kang, T. J. Meyer, *J. Am. Chem. Soc.* **2013**, *135*, 2048–2051; g) T. Zhang, C. Wang, S. Liu, J.-L. Wang, W. Lin, *J. Am. Chem. Soc.* **2014**, *136*, 273–281; h) X.-J. Su, M. Gao, L. Jiao, R.-Z. Liao, P. E. M. Siegbahn, J.-P. Cheng, M.-T. Zhang, *Angew. Chem. Int. Ed.* **2015**, *54*, 4909–4914; *Angew. Chem.* **2015**, *127*, 4991–4996.
- Y. Tachibana, L. Vayssieres, J. R. Durrant, *Nat. Photonics* **2012**, *6*, 511–518.

- [7] a) A. Sartorel, M. Bonchio, S. Campagna, F. Scandola, *Chem. Soc. Rev.* **2013**, *42*, 2262–2280; b) A. Magnuson, M. Anderlund, O. Johansson, P. Lindblad, R. Lomoth, T. Polivka, S. Ott, K. Stensjö, S. Styring, V. Sundström, L. Hammarström, *Acc. Chem. Res.* **2009**, *42*, 1899–1909.
- [8] A. Machkour, D. Mandon, M. Lachkar, R. Welter, *Inorg. Chem.* **2004**, *43*, 1545–1550.
- [9] S. Maji, L. Vigara, F. Cottone, F. Bozoglian, J. Benet-Buchholz, A. Llobet, *Angew. Chem. Int. Ed.* **2012**, *51*, 5967–5970; *Angew. Chem.* **2012**, *124*, 6069–6072.
- [10] a) B. Das, A. Orthaber, S. Ott, A. Thapper, *Chem. Commun.* **2015**, *51*, 13074–13077.
- [11] a) D. Shevchenko, M. F. Anderlund, A. Thapper, S. Styring, *Energy Environ. Sci.* **2011**, *4*, 1284–1287; b) H.-Y. Wang, J. Liu, J. Zhu, S. Styring, S. Ott, A. Thapper, *Phys. Chem. Chem. Phys.* **2014**, *16*, 3661–3669.
- [12] H.-Y. Wang, E. Mijangos, S. Ott, A. Thapper, *Angew. Chem. Int. Ed.* **2014**, *53*, 14499–14502; *Angew. Chem.* **2014**, *126*, 14727–14730.
- [13] G. L. Elizarova, L. G. Matvienko, N. V. Lozhkina, V. N. Parmon, K. I. Zamar-aeu, *React. Kinet. Catal. Lett.* **1981**, *16*, 191–194.
- [14] The potential for the onset of the catalytic wave is taken as the point where the current is 10% of the biggest catalytic peak; see: F. Maillard, A. Bonnefont, M. Chatenet, L. Guetaz, B. Doisneati-Cottignies, H. Rous-sel, U. Stimming, *Electrochim. Acta* **2007**, *53*, 811–822.
- [15] P. Zhang, M. Wang, Y. Yang, T. Yao, L. Sun, *Angew. Chem. Int. Ed.* **2014**, *53*, 13803–13807; *Angew. Chem.* **2014**, *126*, 14023–14027.
- [16] a) J. M. Saveant, E. Vianello, *Electrochim. Acta* **1965**, *10*, 905–920; b) A. J. Bard, L. R. Faulkner, *Electrochemical Methods: Fundamentals and Applications*, John Wiley & Sons, Inc., New York, **2001**.
- [17] a) D. J. Wasylenko, C. Ganesamoorthy, B. D. Koivisto, M. A. Henderson, C. P. Berlinguette, *Inorg. Chem.* **2010**, *49*, 2202–2209; b) D. J. Wasylenko, C. Ganesamoorthy, J. Borau-Garcia, C. P. Berlinguette, *Chem. Commun.* **2011**, *47*, 4249–4251; c) L. Bernet, R. Lalrempuia, W. Ghattas, H. Mueller-Bunz, L. Vigara, A. Llobet, M. Albrecht, *Chem. Commun.* **2011**, *47*, 8058–8060.

Received: October 10, 2015

Published online on January 7, 2016